



Research article

HIF1A-dependent overexpression of MTFP1 promotes lung squamous cell carcinoma development by activating the glycolysis pathway

Jing Ji¹, Yasong Wang¹, Aixin Jing¹, Ling Ma¹, Jiayan Yang¹, Dexu Ren, Jinyu Lv, Mingxiao Lv, Menghan Xu, Qing Yuan, Xinhui Ma, Qilan Qian, Weiling Wang, Ting Geng, Yuanyuan Ding, Jingting Qin, Yuanyuan Liu, Jiaojiao Zhou, Lingyi Zuo, Shaojie Ma^{**}, Xiujun Wang^{***}, Bin Liu^{*}

Jiangsu Key Laboratory of Marine Pharmaceutical Compound Screening, College of Pharmacy, Jiangsu Ocean University, Lianyungang, 222005, China



ARTICLE INFO

Keywords:

Lung squamous cell carcinoma
MTFP1
HIF1A
Glycolysis
Proliferation
Migration

ABSTRACT

Introduction: Mitochondrial fission process 1 (*MTFP1*) is an inner mitochondrial membrane (IMM) protein implicated in the development and progression of various tumors, particularly lung squamous cell carcinoma (LUSC). This study aims to provide a more theoretical basis for the treatment of LUSC.

Methods: Through bioinformatics analysis, *MTFP1* was identified as a novel target gene of *HIF1A*. *MTFP1* expression in LUSC was examined using The Cancer Genome Atlas (TCGA), Gene Expression Omnibus (GEO), and Proteomics Data Commons (PDC) databases. The Kaplan-Meier plotter (KM plotter) database was utilized to evaluate its correlation with patient survival. Western blot and chromatin immunoprecipitation (ChIP) assays were employed to confirm the regulatory relationship between *MTFP1* and *HIF1A*. Additionally, cell proliferation, colony formation, and migration assays were conducted to investigate the mechanism by which *MTFP1* enhances LUSC cell proliferation and metastasis.

Results: Our findings revealed that *MTFP1* overexpression correlated with poor prognosis in LUSC patients ($P < 0.05$). Moreover, *MTFP1* was closely associated with hypoxia and glycolysis in LUSC ($R = 0.203$; $P < 0.001$, $R = 0.391$; $P < 0.001$). *HIF1A* was identified as a positive regulator of *MTFP1*. Functional enrichment analysis demonstrated that *MTFP1* played a role in controlling LUSC cell proliferation. Cell proliferation, colony formation, and migration assays indicated that *MTFP1* promoted LUSC cell proliferation and metastasis by activating the glycolytic pathway ($P < 0.05$).

* Corresponding author. Jiangsu Key Laboratory of Marine Pharmaceutical Compound Screening, College of Pharmacy, Jiangsu Ocean University, Lianyungang, 222005, China.

** Corresponding author. Jiangsu Key Laboratory of Marine Pharmaceutical Compound Screening, College of Pharmacy, Jiangsu Ocean University, Lianyungang, 222005, China.

*** Corresponding author. Jiangsu Key Laboratory of Marine Pharmaceutical Compound Screening, College of Pharmacy, Jiangsu Ocean University, Lianyungang, 222005, China.

E-mail addresses: msjgdp@126.com (S. Ma), wangxiujun@jou.edu.cn (X. Wang), liubin@jou.edu.cn (B. Liu).

¹ These authors contributed equally.

<https://doi.org/10.1016/j.heliyon.2024.e28440>

Received 2 April 2023; Received in revised form 18 March 2024; Accepted 19 March 2024

Available online 21 March 2024

2405-8440/© 2024 Published by Elsevier Ltd.

This is an open access article under the CC BY-NC-ND license

(<http://creativecommons.org/licenses/by-nc-nd/4.0/>).

Conclusions: This study establishes *MTFP1* as a novel *HIF1A* target gene that promotes LUSC growth by activating the glycolytic pathway. Investigating *MTFP1* may contribute to the development of effective therapies for LUSC patients, particularly those lacking targeted oncogene therapies.

1. Introduction

Lung cancer is currently the leading cause of cancer-related deaths worldwide, and is mainly divided into two categories according to pathology: non-small cell lung cancer (NSCLC) and small cell lung cancer (SCLC), with NSCLC accounting for 80% [1]. Lung squamous cell carcinoma (LUSC) is the main pathological subtype of NSCLC and has characteristics of poor prognosis and high recurrence rate [2]. However, traditional treatment methods have many limitations [3]. In recent years, molecular targeted therapy has brought new hopes to patients with lung squamous cell carcinoma [4]. It is essential to find specific biological markers for targeted therapy of lung squamous cell carcinoma and to confirm their roles and mechanisms of action, in order to develop more effective treatment strategies.

Mitochondria are the most main oxygen-consuming organelles in cells and are the core sites of cellular metabolism, providing sufficient energy and materials for cells [5]. Solid tumors often have low oxygen levels in their core regions due to rapid growth. Mitochondria in tumor cells often undergo changes in quantity, structure and function in order to adapt to the rapid growth of tumors in acidic and hypoxic environments [6]. Mitochondrial fission increases can promote the production of reactive oxygen species (ROS) in cells, thus promoting tumorigenesis and development [7]. Mitochondrial fission process 1 (*MTFP1*) is a mitochondrial membrane protein that participates in the promotion of mitochondrial fission and plays an important role in cell vitality and mitochondrial dynamics [8]. Studies have shown that *MTFP1* overexpression can induce ROS production and promote the growth of oral squamous cell carcinoma [9]. In hepatocellular carcinoma, high expression of *MTFP1* can promote the growth and metastasis of hepatocellular carcinoma cells by inducing G1 to S phase transition of cells and inhibiting apoptosis [10]. In addition, classical tumor suppressor P53 can reduce Drp1-driven mitochondrial fission by inhibiting *MTFP1* protein expression mediated by mTORC1 [11]. This regulation mechanism allows P53 to limit cell migration and invasion controlled by Drp1-mediated mitochondrial fission. In addition, there are reports that there is a certain relationship between *MTFP1* and hypoxia [12]. These studies all indicate that *MTFP1* may play an important role in tumors. However, it is still unclear whether *MTFP1* expression is beneficial to the growth of lung squamous cell carcinoma cells.

Based on this, we found abnormal overexpression of *MTFP1* in LUSC by bioinformatics analysis, and will further experimentally explore the biological function and mechanism of *MTFP1* in the development of lung squamous cell carcinoma. This study aims to provide a more theoretical basis for a novel therapeutic target for patients with lung squamous cell carcinoma who lack oncogene targeted therapy and may contribute to the development of effective treatments for this disease.

2. Materials and methods

2.1. Data collection and analysis

MTFP1 mRNA expression levels in pan-cancer and adjacent normal tissues, as well as lung squamous cell carcinoma and normal lung tissues were obtained from the GEPIA2 online tool (<http://gepia2.cancer-pku.cn>). The microarray data of GSE158632 (platform: GPL21697), GSE33532 (platform: GPL570) and GSE136043 (platform: GPL13497) were retrieved from the Gene Expression Omnibus (GEO) database. GSE33532 included two CoCl₂-treated cells, GSE33532 included 80 lung squamous cell carcinoma samples and 20 normal samples, while GSE136043 contained 5 lung squamous cell carcinoma samples and 5 normal samples. Transcriptome data were normalized with the "limma" package for differential analysis in R-4.1.0.

The mRNA levels of *MTFP1* in GSE33532 and GSE136043 were plotted using GraphPad Prism 9 software. The *MTFP1* mRNA expression levels in patients with different clinical-pathological groups in LUSC were obtained from the UALCAN online tool (<http://ualcan.path.uab.edu>). The protein expression data of *MTFP1* in normal lung tissues and lung squamous cell carcinoma samples were obtained from the Proteomic Data Commons (PDC) database.

The correlation between *MTFP1* mRNA expression and overall survival (OS), free-progression survival (FPS) and post-progression survival (PPS) in patients with LUSC was evaluated using the Kaplan Meier - plotter (KM plotter) database (<http://kmplot.com/analysis>). The correlation between *MTFP1* and the hypoxia signature gene set, as well as *LDHA*, *HK2*, *GLUT1*, and *PKM2* in LUSC, was analyzed using the GEPIA2 online tool. The correlation between *MTFP1* and *ENO1*, *PGK1* and *PDK1*, as well as the correlation between *MTFP1* and glycolysis and oxidative phosphorylation were analyzed by the spearman method in R-4.1.0. The "ggplot2" R package was used for plotting.

The promoter sequence of *MTFP1* was obtained from the EPD online database (<https://epd.epfl.ch/>). The HREs in the promoter region of *MTFP1* were predicted using the JASPAR online database (<https://jaspar.genereg.net/>). Gene Ontology (GO) analysis was performed using the "enrichment GO" function in the R package "clusterProfiler". The "enrichment KEGG" function was used for the Kyoto Encyclopedia of Genes and genomes (KEGG) analysis.

According to the expression of *MTFP1* in TCGA-LUSC samples, the TCGA-LUSC samples were divided into the *MTFP1*-high group and the *MTFP1*-low group. Gene Set Enrichment Analysis (GSEA) was performed using the Hallmark Gene Set (<http://www.gsea->

msigdb.org/) and R packages "fgsea", "Enrichment plot", "gggsea" and "clusterProfiler" in R-4.1.0.

2.2. Cell culture

HEK293T cells and LUSC cell lines NCI-H2170 and NCI-H520 cells were purchased from American Type Culture Collection (ATCC). Cells were cultured in DMEM high glucose or RPMI-1640 medium supplemented with 10% FBS (Gibco), 100 U/mL penicillin, and 100 U/mL streptomycin (Gibco). For the physical hypoxia model, NCI-H2170 and NCI-H520 cells were cultured for 24 h in a hypoxic incubator with 1% oxygen. For the chemical hypoxia model, NCI-H2170 and NCI-H520 cells were treated with 200 μ mol/L cobalt chloride for 24 h.

2.3. RNA isolation, real-time PCR and RNA interference

Trizol reagent (Invitrogen, USA) was used to extract the total RNA from human lung adenocarcinoma cells. The mRNA is then transcribed into cDNA using the reverse transcription kit (Promega, USA). Real-time PCR was performed on Light Cycler 480 (Roche, Switzerland). GAPDH was used as an internal control. Differences in gene expression were calculated using the $2^{-\Delta\Delta Ct}$ method and expressed as fold-changes. Primers were listed as follows: *MTFP1* forward, 5'- TGTGGTGGACACCTTGTATGG -3'; reverse, 5'- TGGGGTGGATAATGATGGGGA-3'; *GAPDH* forward, 5'- TGTGGGCAT- CAATGGATTTGG -3'; reverse, 5'- ACACCATGTATTCCGGGT- CAAT-3'; The short hairpin RNA (sh-RNA)-expressing plasmids were purchased from Merck-Sigma.

2.4. MTT assay

Cell viability was determined by using the 3-(4,5-dimethylthiazol-2-yl)-2,5-diphenyltetrazolium bromide (MTT; Sigma, St Louis, USA) colorimetric assay. Briefly, cells were seeded in 96-well plates and incubated for 24 h, and cells were subject to different treatment regimens. After the treatments, cells were washed with phosphatebuffered saline (PBS) and then incubated in MTT solution (Sigma) for 3 h. After dimethyl sulfoxide was added into each well, the absorbance was measured at 490 nm to determine the cell viability with a microplate reader (BioTek, Winooski, USA).

2.5. Western blotting and antibodies

Cells were lysed in SDS loading buffer. The boiled samples were separated by 12% SDS-PAGE and transferred to nitrocellulose membranes. The membranes were blocked with 5% non-fat milk, and incubated with indicated antibodies overnight at 4 °C. The membranes were then washed with PBS followed by incubation with secondary antibodies for 45 min. The signals of the proteins were visualized on an ImageQuant LAS 4000 system (GE Healthcare). The primary antibodies used in this study including anti-MTFP1 (Abclonal, china) and anti - actin (Santa Cruz, USA).

2.6. Chromatin immunoprecipitation (ChIP) assay

ChIP assay using a chromatin immunoprecipitation assay kit (Millipore, USA) according to the manufacturer's instructions. Cells were fixed with 1% formaldehyde and lysed with SDS lysis buffer. The DNA was sheared into 200–600 bp fragments by ultrasound. The lysate containing soluble chromatin was incubated and precipitated overnight with the indicated antibodies, including anti-GAPDH (Santa Cruz, USA), anti-MTFP1 (Abclonal, china) Or rabbit IgG (#ab172730, Abcam). Then the Protein A/G Sepharose was added for additional 4 h. Protein-DNA crosslinking was then reversed by treating with proteinase K at 45 °C for 2 h. The DNA was then purified, diluted and subjected to a real-time PCR reaction.

2.7. Xenograft assays

All animal experiments were approved by the Institutional Animal Ethics Committee of Jiangsu Ocean University, and animal care was in accordance with institutional guidelines. 6-week-old male nude mice were kept in a facility free of specific pathogens. Con-shRNA or *MTFP1*-shRNA cells with a density of 5×10^6 were suspended in 50 μ L DMEM medium, mixed with Matrigel (Corning; 1:1), and then injected into the ventral side of each nude mice. The size of the tumor was measured with a caliper every week. The tumor volume was calculated using the formula length \times width $2 \times 1/2$. Four weeks after the injection, the mice were sacrificed by cervical dislocation, and the tumor weight was measured and photographed.

2.8. Glucose, lactic acid, and ATP detection

To detect glucose utilization, lactic acid production, and intracellular ATP production, we utilized the glucose detection kit, lactic acid detection kit, and ATP detection kit (Beyotime, China) in accordance with the manufacturer's instructions.

2.9. Cell proliferation assay

For cell proliferation assay, cells were seeded uniformly in 96-well plates at a density of 10,000 cells/well, and five multiple wells

were established for each group. After cell attachment, the CCK-8 kit was used to measure cell proliferation according to the manufacturer’s instructions. Ten microliters of CCK-8 reagent were added to each well, followed by incubation for 2 h. The absorbance values were measured at 450 nm using an enzyme marker. For the bromodeoxyuridine (BrdU) incorporation assay, cells were seeded in 96-well plates containing 10 μmol/L BrdU solution. After 24 h, cells were fixed in PBS containing 4% paraformaldehyde for 20 min. Subsequently, cells were washed with PBS and treated with DNase at room temperature for 15 min. BrdU antibody and TMB substrate were then added, and cells were incubated. The absorbance was measured at 450 nm using a microplate reader.

2.10. Colony formation

Cells in good growth condition were seeded uniformly into 12-well plates at a density of 1000 cells/well. The plates were then incubated at 37 °C in a 5% CO₂ incubator for 10–14 days. After the colonies were visible to the naked eye, they were fixed in 4% paraformaldehyde for 15 min and stained with crystal violet for 30 min. The colonies were then photographed and counted.

2.11. Cell invasion

Matrigel and DMEM were mixed and added to the upper Transwell chamber, followed by incubation at 37 °C for 30 min. A total of 100 μL of cell suspension (5 × 10⁴ cells/well) was then added to the matrigel. Six hundred microliters of chemotactic solution were added to the lower chamber, and the Transwell plates were cultured in a 5% CO₂ cell incubator at 37 °C for 24 h. The uninvaded cells were removed with a cotton swab, and the invaded cells were fixed with paraformaldehyde for 20 min and stained with crystal violet for 30 min. After washing with PBS and drying, the stained cells were counted under a microscope, and the number of cells in five fields was averaged.

2.12. Statistical analysis

The data are presented as mean ± standard deviation (SD). Statistical analysis was performed using R-4.1.0 and GraphPad Prism 9.0. The differences between groups were determined using the student’s t-test (for comparisons of two groups) or one-way ANOVA.

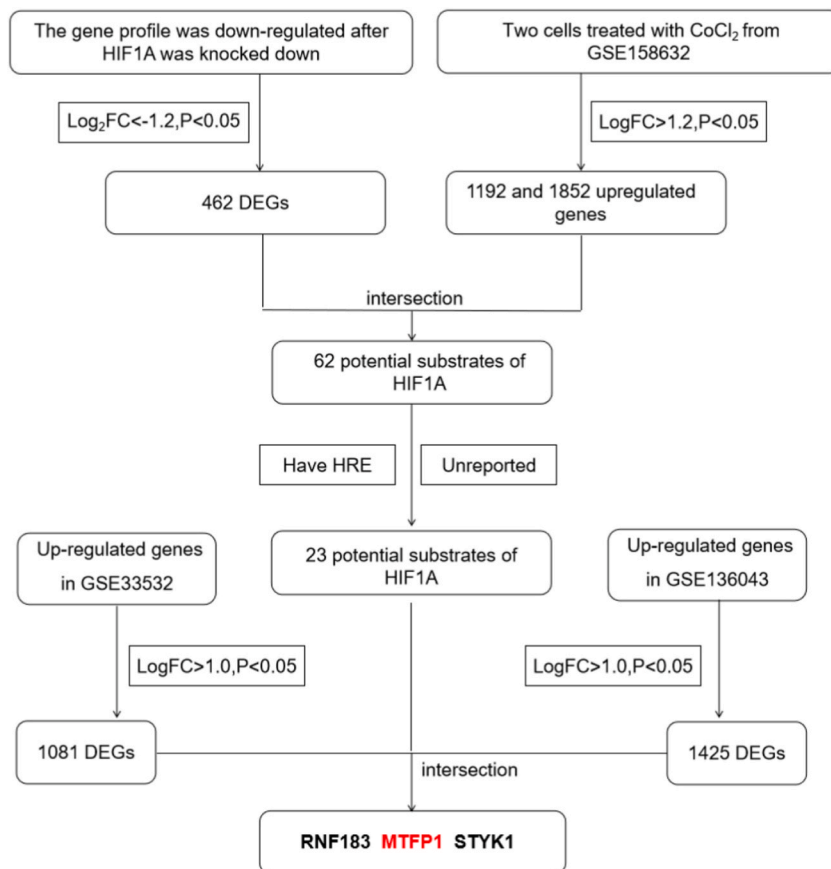


Fig. 1. MTFP1 flow diagram of bioinformatics analysis of the study.

The p-value <0.05 was considered statistically significant and was expressed as * $P < 0.05$, ** $P < 0.01$, and *** $P < 0.001$, respectively.

3. Results

3.1. Overexpression of *MTFP1* in LUSC was associated with a poor prognosis

First, we analyzed the *HIF1A* knockout gene expression data (Supplementary Table 8) and CoCl2 processing two cell gene expression data (Supplementary Table 9 and 10), got 62 potential *HIF1A* substrates (Supplementary Table 11). Then, by bioinformatics analysis, we found that *MTFP1* overexpression was associated with poor prognosis in LUSC (Fig. 1). To investigate the role of *MTFP1* in cancers, we used the GEPIA2 online tool to examine the expression of *MTFP1* mRNA in 33 different human tumor types and their

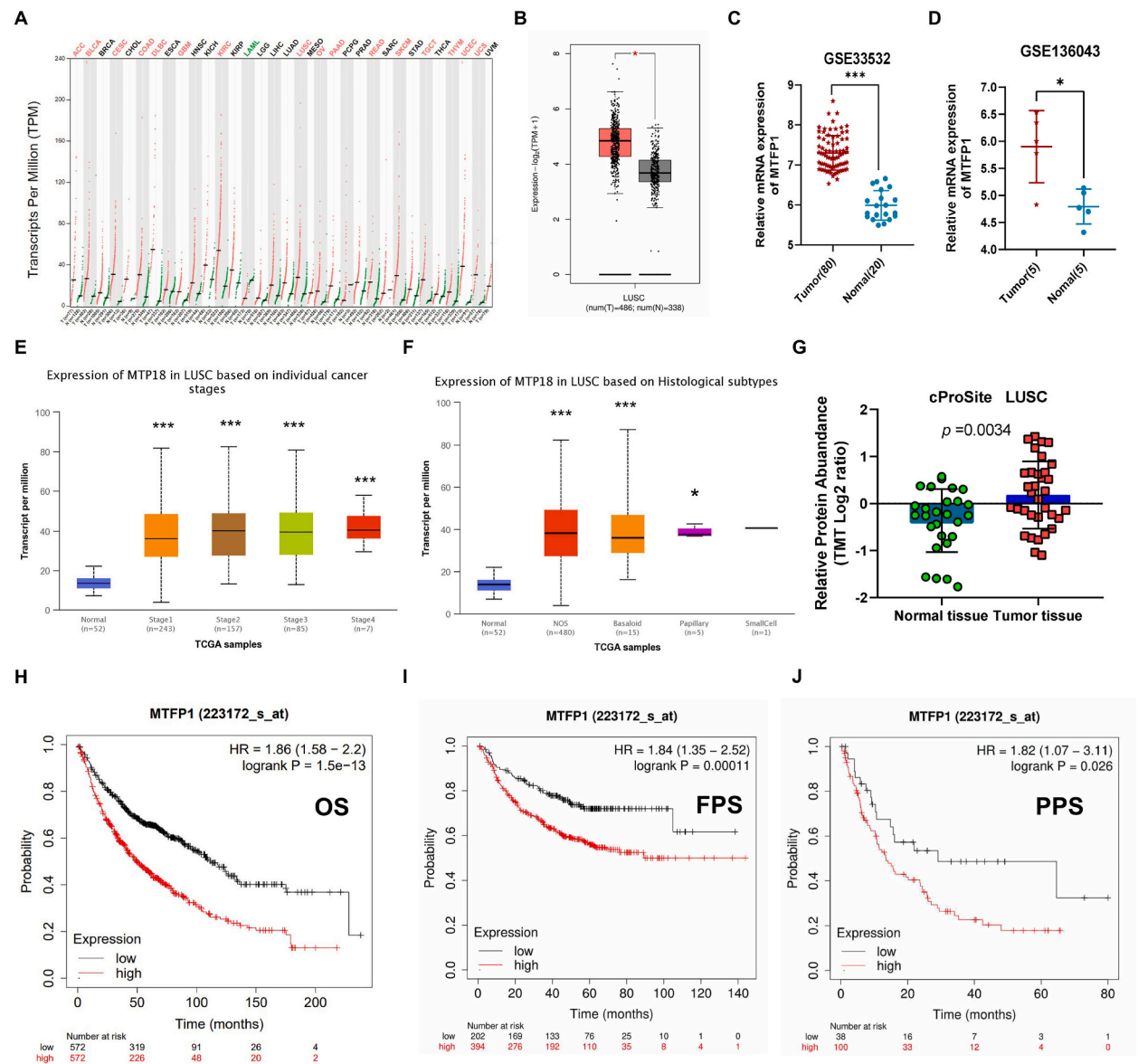


Fig. 2. Overexpression of *MTFP1* in LUSC was associated with a poor prognosis (A) GEPIA2 online tool was used to plot the mRNA expression of *MTFP1* in pan-carcinoma and corresponding adjacent normal tissues. (B) mRNA expression of *MTFP1* was analyzed in 486 squamous cell lung carcinoma samples and 338 normal samples from both TCGA and GTEx databases. (C, D) *MTFP1* mRNA expression was measured in lung cancer samples and normal samples from GSE33532 and GSE136043, respectively. (E, F) The mRNA expression of *MTFP1* was analyzed in different stages and subtypes of LUSC. (G) Protein expression of *MTFP1* was measured in normal lung tissue and LUSC samples from the CPTAC database. (H–J) The overall survival (OS), free-progression survival (FPS), and post-progression survival (PPS) curves of *MTFP1* expression in squamous cell lung carcinoma patients. * $P < 0.05$, *** $P < 0.001$. Data were analyzed using Student’s *t*-test.

corresponding normal tissues. Our results showed that *MTFP1* mRNA expression was considerably higher in tumor tissues compared to normal tissues in approximately 50% (16/33) of the cancer types (Fig. 2A). Furthermore, lung squamous cell carcinoma (LUSC) tissues continued to express *MTFP1* at a level that was considerably higher than that of healthy controls, even after incorporating GTEx data (Fig. 2B). Consistent with our findings, analysis of the GSE33532 and GSE136043 datasets (Supplementary Table 1 and 2) further demonstrated that *MTFP1* expression was higher in LUSC samples than in normal samples (Fig. 2C–D). Subsequent analysis using the UALCAN online tool revealed that mid-late-stage LUSC tissues had significantly higher levels of *MTFP1* expression than early-stage tissues (Fig. 2E). Additionally, we observed that *MTFP1* expression was higher in three other types of lung cancer compared to healthy lung tissues (Fig. 2F), indicating that *MTFP1* plays a role in the development of multiple types of lung cancer. Correspondingly, in the CPTAC database, we observed greater levels of *MTFP1* protein expression in LUSC samples than in healthy lung tissues (Fig. 2G). To investigate the clinical significance of *MTFP1* in LUSC, we used the Kaplan-Meier Plotter tool to assess the relationship between *MTFP1* transcription levels and patient survival. Our data revealed that high expression of *MTFP1* was negatively correlated with overall survival (OS), free-progression survival (FPS), and post-progression survival (PPS) of LUSC patients (Fig. 2H–J), indicating that *MTFP1* overexpression is associated with a poor prognosis in LUSC.

3.2. *MTFP1* is closely related to hypoxia and glycolysis

Previous studies have reported an association between *MTFP1* and hypoxia, and it is well established that hypoxic environments

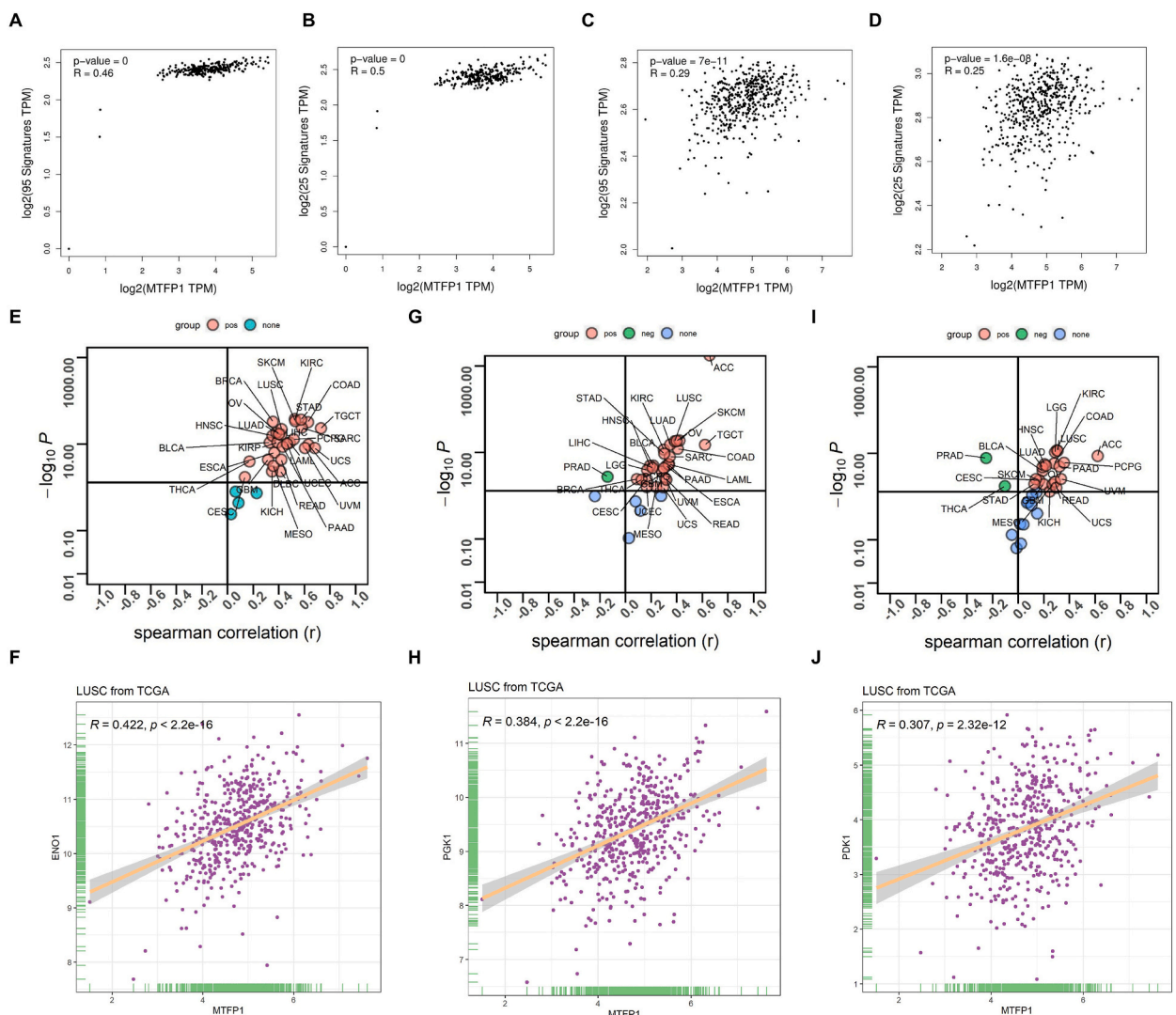
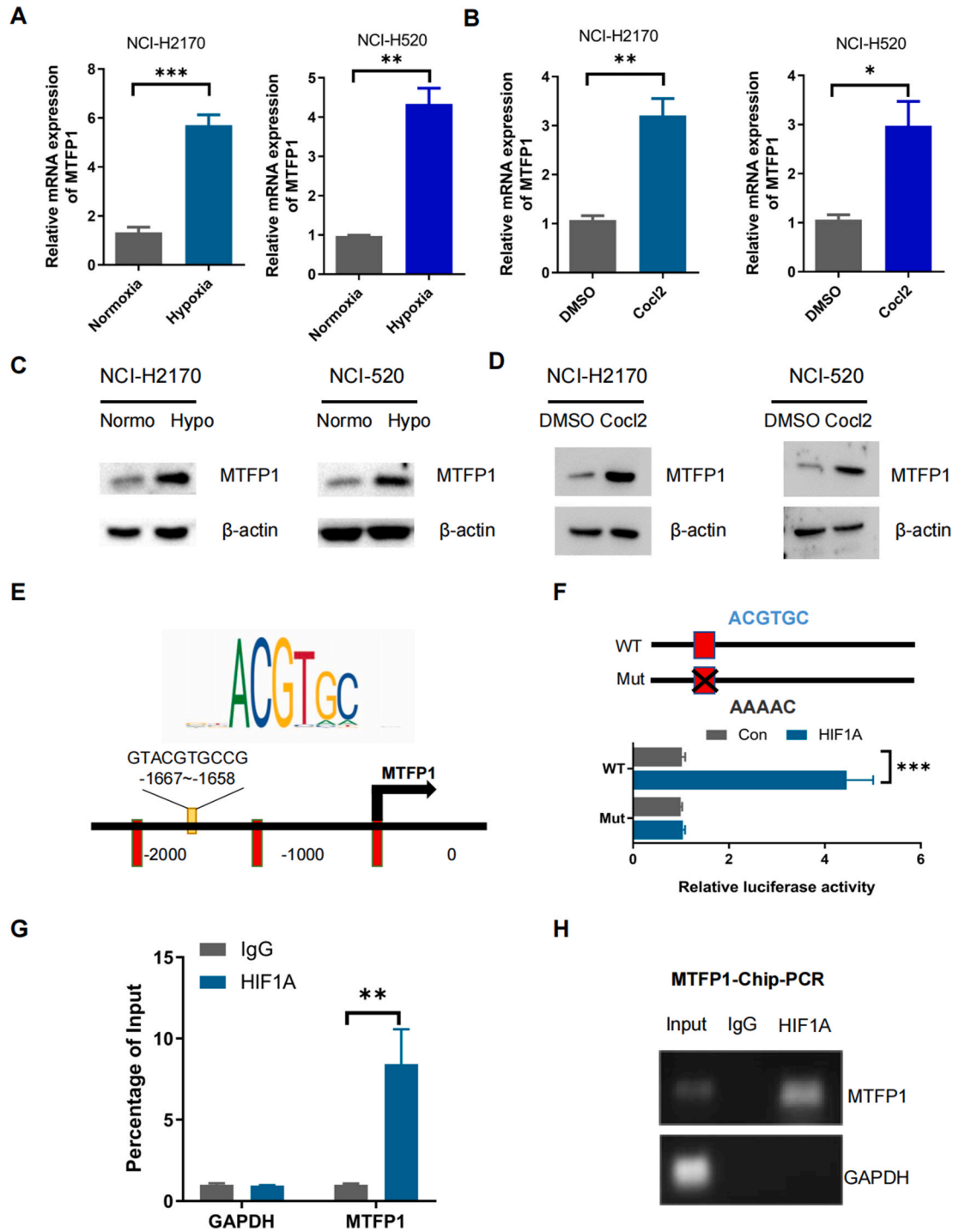


Fig. 3. *MTFP1* is closely related to hypoxia and glycolysis. Scatter plots indicating the correlation between *MTFP1* with 95 and 25 hypoxic metagenes in the GTEx-Lung (A, B) and the TCGA-LUSC database (C, D), respectively. Correlation of *MTFP1* with *ENO1* (E), *PGK1* (G), and *PDK1* (I) in the TCGA tumor database and the TCGA-LUSC database (F, H, J).



(caption on next page)

Fig. 4. *HIF1A* is a positive regulator of *MTFP1* (A, B) Relative expression of *MTFP1* in human lung adenocarcinoma cell lines NCI-H2170 or NCI-H520 after physical hypoxia or cobalt chloride treatment was detected by polymerase chain reaction (PCR). (C, D) Western blotting was used to detect the protein expression of *MTFP1* in human lung adenocarcinoma cells NCI-H2170 or NCI-H520 after physical hypoxia treatment or hypoxic treatment induced by cobalt chloride. *MTFP1* was compared with β -actin. (E) Schematic diagram showing hypothetical response elements from the human *MTFP1* gene promoter. TSS: transcriptional starting point. (F) The human *MTFP1* promoter contains one potential binding site for *HIF1A* was highlighted with RED. The mutant site was labeled with “×”. 293T cells were co-transfected with *HIF1A* and the indicated vector for 36 h, and luciferase activity was detected. (G) ChIP-qPCR assay showed the enrichment of *HIF1A* in the putative *HIF1A* binding site of the *MTFP1* promoter region. (** $P < 0.01$). (H) ChIP-PCR amplification results using primers targeting the *MTFP1* promoter region, and the PCR products were separated by agarose gel electrophoresis.* $P < 0.1$, ** $P < 0.01$, and *** $P < 0.001$. Data were analyzed using Student’s *t*-test. (For interpretation of the references to color in this figure legend, the reader is referred to the Web version of this article.)

promote cancer growth. We carried out an analysis using data from the TCGA and GTEx databases to investigate the correlation between *MTFP1* and hypoxia. Specifically, we analyzed the expression of 95 hypoxia signature genes (Supplementary Table 3) and 25 hypoxia-inducible genes (Supplementary Table 4) in hypoxic tumor cells [13,14]. Our analysis of both normal lung tissue (Fig. 3A–B) and lung squamous carcinoma samples (Fig. 3C–D) revealed a strong correlation between the majority of these genes and *MTFP1*,

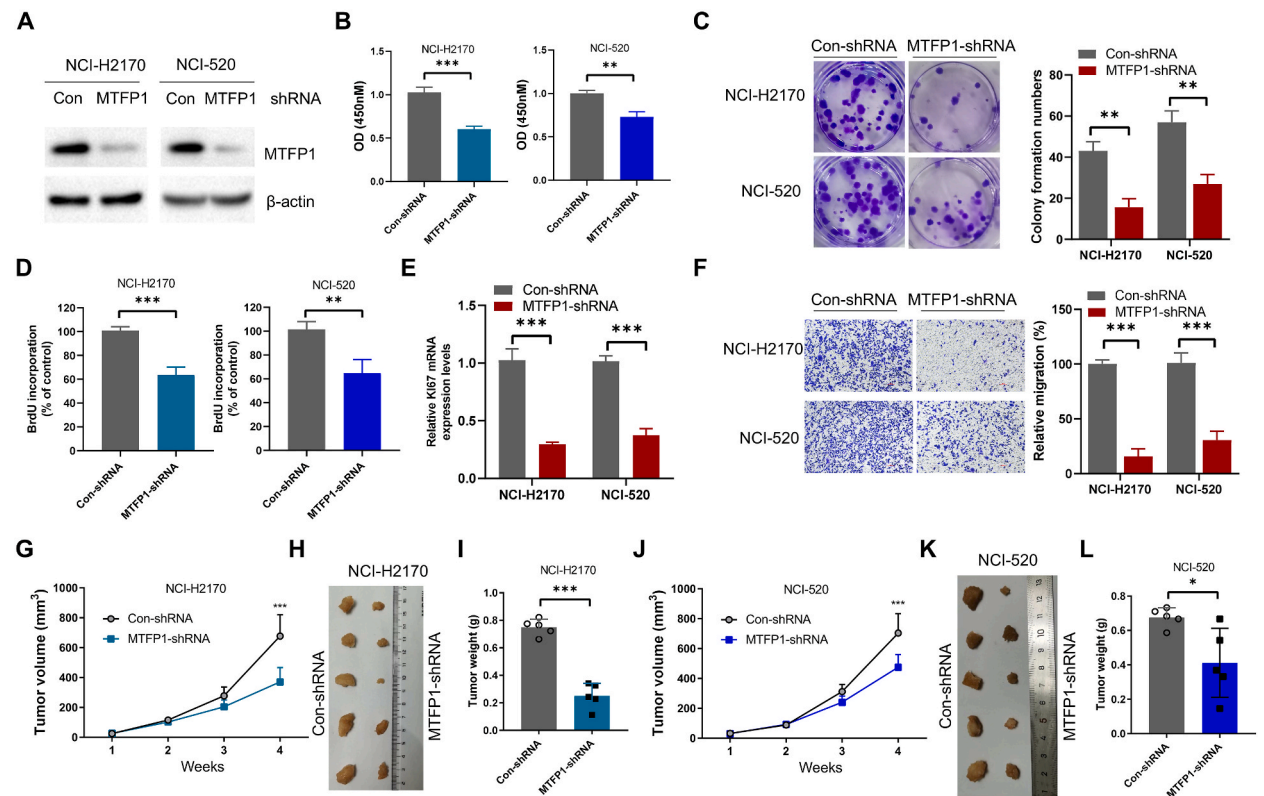


Fig. 5. Knockdown of *MTFP1* inhibited LUSC tumor growth. (A) Western blot analysis was used to assess the expression of *MTFP1* in NCI-H2170 and NCI-520 cells transfected with either control-shRNA or *MTFP1*-shRNA. Beta-actin was used as a loading control. (B) The CCK-8 assay was performed to evaluate the effect of *MTFP1* knockdown on cell proliferation in NCI-H2170 and NCI-520 cells. Cells were transfected with either control-shRNA or *MTFP1*-shRNA for 72 h prior to analysis. (C) Colony formation assay was performed to assess the effect of *MTFP1* knockdown on the ability of NCI-H2170 and NCI-520 cells to form colonies. (D) The ELISA measurement of BrdU incorporation was used to determine the effect of *MTFP1* knockdown on cell proliferation in NCI-H2170 and NCI-520 cells. Cells were transfected with either control-shRNA or *MTFP1*-shRNA for 72 h prior to analysis. (E) Real-time PCR analysis was performed to evaluate the effect of *MTFP1* knockdown on MKI67 mRNA expression in NCI-H2170 and NCI-520 cells. (F) Transwell migration assay was used to evaluate the effect of *MTFP1* knockdown on the ability of NCI-H2170 and NCI-520 cells to migrate. (G) Tumor growth curves were generated to evaluate the effect of *MTFP1* knockdown on LUSC tumor growth in a xenograft mouse model using NCI-H2170 cells with stable *MTFP1* knockdown. (H) Tumors harvested from NCI-H2170 with stable *MTFP1* knockdown were photographed to assess the effect of *MTFP1* knockdown on tumor growth. (I) Statistical analysis was performed to evaluate the effect of *MTFP1* knockdown on tumor size in NCI-H2170 with stable *MTFP1* knockdown. (J) Tumor growth curves were generated to evaluate the effect of *MTFP1* knockdown on LUSC tumor growth in a xenograft mouse model using NCI-520 cells with stable *MTFP1* knockdown. (K) Tumors harvested from NCI-520 with stable *MTFP1* knockdown were photographed to assess the effect of *MTFP1* knockdown on tumor growth. (L) Statistical analysis was performed to evaluate the effect of *MTFP1* knockdown on tumor size in NCI-520 with stable *MTFP1* knockdown. Data are presented as mean \pm SEM of at least three independent experiments. Statistical significance was determined using Student’s *t*-test. * $P < 0.1$, ** $P < 0.01$, and *** $P < 0.001$. Data were analyzed using one-way ANOVA.

suggesting a close association between *MTFP1* and hypoxia. Furthermore, we identified two glycolysis enzymes, *ENO1* and *PGK1*, among these hypoxia signature genes, as glycolysis is closely linked to hypoxia. *ENO1*, *PGK1*, and *PDK1*, a glycolysis regulatory factor regulated by *PGK1*, are characteristic genes in the hypoxia signaling pathway according to the MSigDB database. We therefore further analyzed the correlation between *MTFP1* and these three genes. Our results demonstrate a significant correlation between *MTFP1* and *ENO1* (Fig. 3E–F), *PGK1* (Fig. 3G–H), and *PDK1* (Fig. 3I–J) in most tumor types, including lung squamous carcinoma. These observations suggest a significant association between *MTFP1* and both hypoxia and glycolysis.

3.3. *HIF1A* is a positive regulator of *MTFP1*

To investigate whether hypoxia mediates the upregulation of *MTFP1* in lung squamous cell carcinoma (LUSC), we treated human lung adenocarcinoma cell lines, NCI–H2170 and NCI–H520, with either hypoxia or hypoxia mimetic cobalt chloride. We found that both hypoxia and cobalt chloride significantly induced both *MTFP1* mRNA and protein levels (Fig. 4A–D). Furthermore, we assessed the impact of cobalt chloride treatment on the cell viability of two human lung adenocarcinoma cell lines, namely NCI–H2170 and NCI–H520. Our results revealed a significant increase in cell viability following cobalt chloride treatment as compared to the control group (Fig. S1A). *HIF1A* recognizes hypoxia response elements (HREs) within promoter regions to regulate downstream target gene

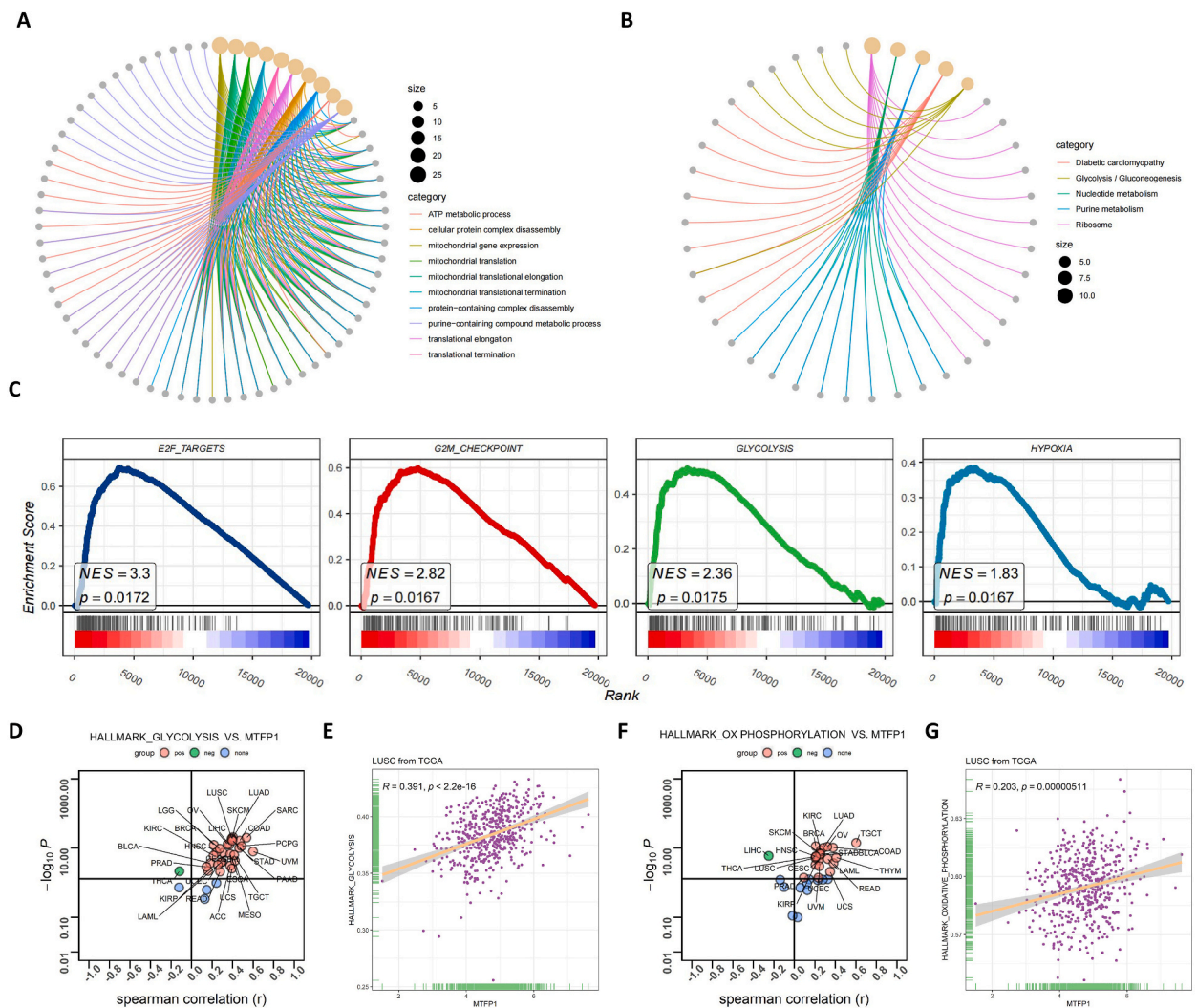


Fig. 6. *MTFP1* was involved in LUSC cell proliferation and energy metabolism. Gene ontology (GO) analysis and (A) Kyoto encyclopedia of genes and genomes (KEGG) analysis (B) based on co-expressed genes in LUSC of *MTFP1*. (C) Gene set enrichment analysis (GSEA) of the E2F targets, G2M checkpoint, glycolysis, and hypoxia signature genes in the *MTFP1*-high group, as compared to the *MTFP1*-low group. (D) Correlation between *MTFP1* and HALLMARK_GLYCOLYSIS in 33 types of human cancer from TCGA. (E) Scatter plots indicating the correlation between *MTFP1* and HALLMARK_GLYCOLYSIS in TCGA-LUSC. (F) Correlation between *MTFP1* and oxidative phosphorylation in 33 types of human cancer from TCGA. (G) Scatter plots indicating the correlation between *MTFP1* and oxidative phosphorylation in TCGA-LUSC.

expression [15]. Applying JASPAR transcription factor prediction database analysis, we observed that the *MTFP1* promoter region contained a canonical HRE (Fig. 4E). In luciferase assays, *HIF1A* significantly promoted the luciferase activity of the wild-type *MTFP1* promoter, but not the mutant-type promoter (Fig. 4F). We then performed ChIP-PCR assays to examine whether *HIF1A* directly binds to the *MTFP1* promoter, and observed that the *MTFP1* promoter could be efficiently recovered from *HIF1A* immunoprecipitates, but not from control immunoprecipitates, indicating that *HIF1A* directly binds to the *MTFP1* promoter region (Fig. 4G–H). Therefore, we conclude that *MTFP1* is a direct target of *HIF1A* in LUSC, where the expression of *MTFP1* is induced by hypoxia, and *HIF1A* directly binds to its promoter region containing an HRE.

3.4. Knockdown of *MTFP1* inhibited LUSC tumor growth

The previous results suggest that *MTFP1* plays a crucial role in LUSC. To investigate this further, we generated stable *MTFP1*-

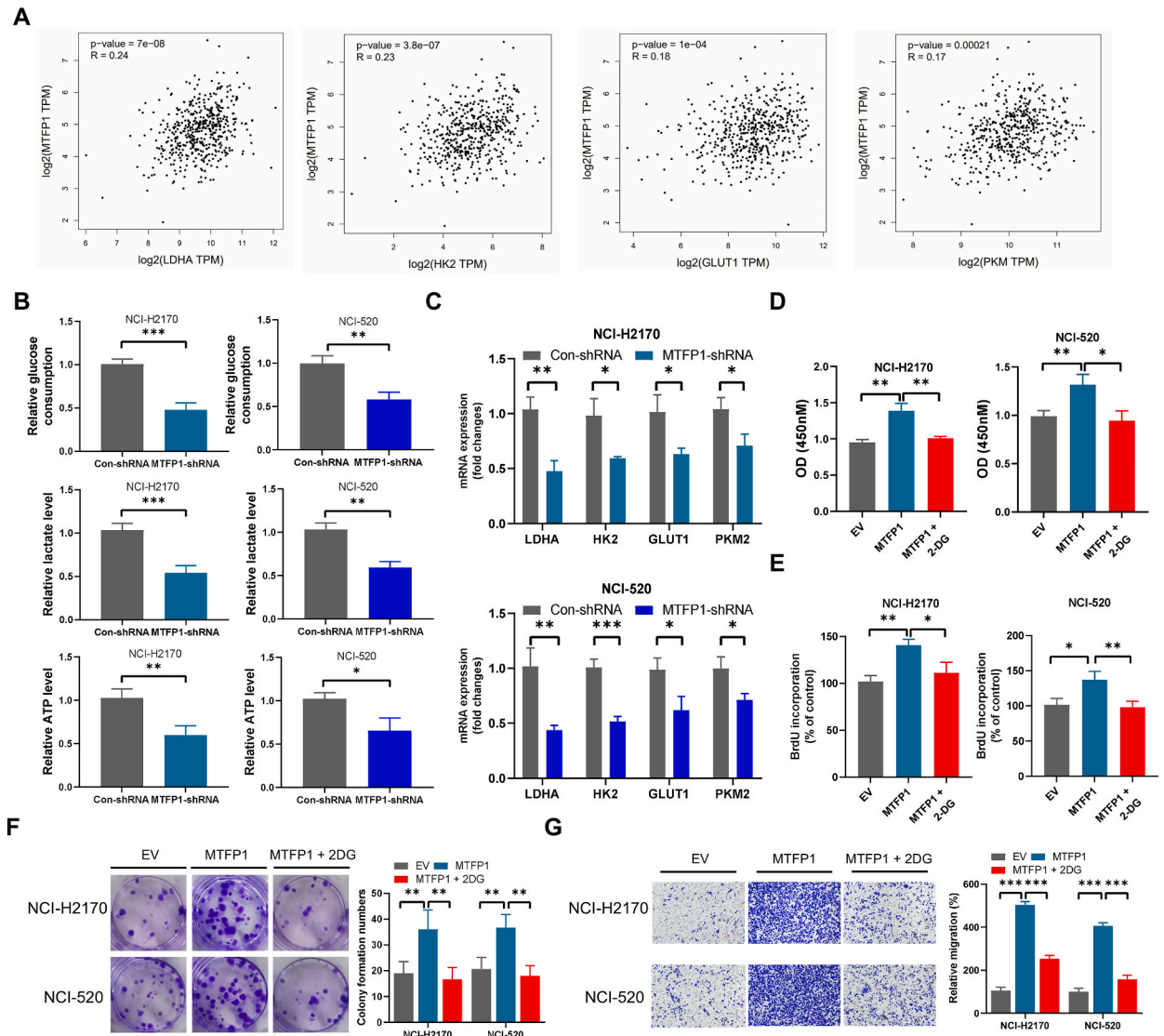


Fig. 7. *MTFP1* promoted the proliferation and migration of LUSC by regulating glycolysis. Correlation between *MTFP1* and *LDHA*, *HK2*, *GLUT1*, and *PKM2* mRNA expression levels in the TCGA database, as analyzed by GEPIA2. (B) Relative glucose consumption, lactate production, and ATP levels in NCI-H2170 and NCI-520 cells with stable *MTFP1* knockout. (C) mRNA expression levels of *LDHA*, *HK2*, *GLUT1*, and *PKM2* in NCI-H2170 and NCI-520 cells with stable *MTFP1* knockout, as determined by RT-qPCR. (D) Proliferation ability of NCI-H2170 and NCI-520 cells overexpressing *MTFP1* or treated with 2DG, as measured by CCK-8 assay. (E) Quantification of BrdU-positive cells in NCI-H2170 and NCI-520 cells overexpressing *MTFP1* or treated with 2DG. (F) Images of cell colonies and quantification of colony numbers from the experiment shown in (D). (G) Representative images and quantification of transwell migration assay of cells shown in (D). Data are presented as mean \pm SEM of at least three independent experiments. * $P < 0.1$; ** $P < 0.01$; *** $P < 0.001$. Data were analyzed using one-way ANOVA.

knockdown cell lines by transducing NCI-H2170 and NCI-520 LUSC cells with Con-shRNA and *MTFP1*-shRNA lentiviruses. Western blotting confirmed the knockdown efficiency (Fig. 5A). CCK8 assay revealed that *MTFP1* knockdown significantly reduced the growth of NCI-H2170 and NCI-520 cells (Fig. 5B), as well as their colony-forming ability (Fig. 5C). The 5-bromo-2'-deoxyuridine (BrdU) incorporation assay further demonstrated reduced proliferation in *MTFP1*-knockdown NCI-H2170 and NCI-520 cells (Fig. 5D). Furthermore, qRT-PCR analysis showed that *MTFP1* knockdown resulted in significant downregulation of the cell proliferation-related gene *KI67* (Fig. 5E). The cell migration assay also demonstrated that *MTFP1* knockdown weakened the migration ability of the two LUSC cell lines (Fig. 5F), suggesting that *MTFP1* regulates LUSC cell proliferation and migration.

We also investigated whether *MTFP1* promotes LUSC tumor growth. Stable *MTFP1*-knockdown NCI-H2170 and NCI-520 cells were subcutaneously injected into nude mice to establish xenograft models. Compared with the control group, *MTFP1*-knockdown NCI-H2170 cells showed weakened tumor growth, with significantly smaller tumor volume and weight (Fig. 5G–I). Similarly, *MTFP1* knockdown in NCI-520 cells resulted in significant inhibition of tumor growth (Fig. 5J–L). In conclusion, these in vitro and in vivo experimental results demonstrate that *MTFP1* knockdown reduces LUSC cell proliferation and suppresses tumor growth.

3.5. *MTFP1* was involved in LUSC cell proliferation and energy metabolism

Analyzing the co-expression network can provide insight into the biological functions of a gene. We searched for the top 1000 co-expressed genes with *MTFP1* from two online databases, cBioPortal and Coexpressdb (Supplementary Tables 5 and 6), and identified 186 common genes (Supplementary Table 7). GO analysis revealed that *MTFP1* is associated with ATP metabolic processes (Fig. 6A), while KEGG analysis showed that *MTFP1* is involved in the glycolysis process (Fig. 6B), indicating its participation in cellular energy metabolism. Additionally, based on the expression of *MTFP1* in TCGA-LUSC samples, we divided them into high-expression and low-expression groups for GSEA analysis. Pathways related to cell proliferation and energy metabolism, such as E2F targets, G2M checkpoint, glycolysis, and hypoxia, were significantly enriched in the *MTFP1* high-expression group (Fig. 6C). Therefore, we further analyzed the correlation between *MTFP1* and glycolysis and oxidative phosphorylation. The results showed that *MTFP1* was positively correlated with glycolysis in most tumors (28/33) (Fig. 6D). In addition, a significant correlation was observed between *MTFP1* mRNA levels and glycolysis in LUSC (Fig. 6E), while a good correlation was observed between *MTFP1* mRNA levels and oxidative phosphorylation in LUSC (Fig. 6F–G). These findings suggest that *MTFP1* may play a role in the regulation of energy metabolism in LUSC, in addition to its involvement in cell proliferation.

3.6. *MTFP1* promoted the proliferation and migration of LUSC by regulating glycolysis

To examine the correlation between *MTFP1* and four key molecules in the glycolytic pathway of LUSC, we used GEP1A2 online tool and found a significant positive correlation between *MTFP1* and *LDHA*, *HK2*, *GLUT1*, and *PKM2* (Fig. 7A). We further assessed the impact of *MTFP1* on glycolysis in LUSC cells and found that *MTFP1* expression suppression led to reduced glucose consumption, lactate

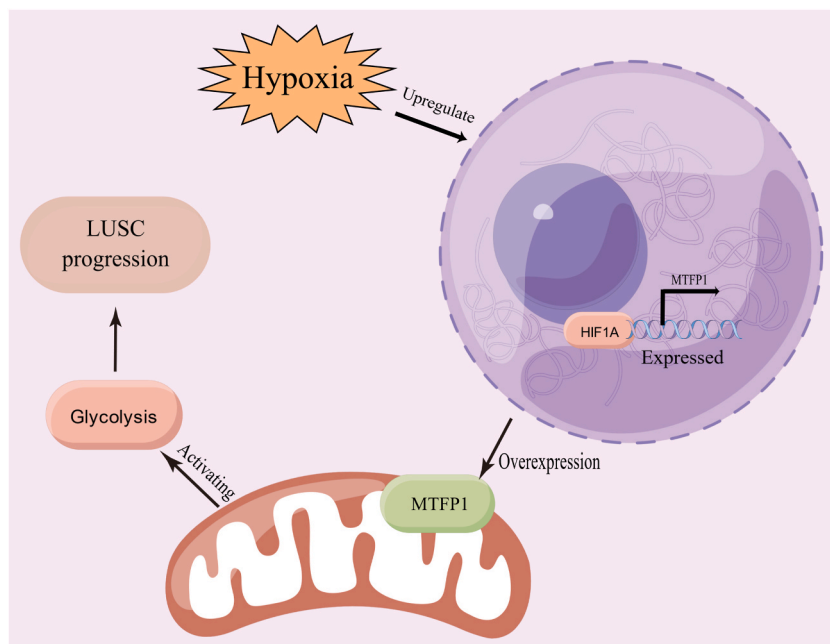


Fig. 8. Schematic diagram of the mechanistic link between increased *HIF1A* expression induced by hypoxia positively regulates *MTFP1* overexpression and regulates glycolytic to promote proliferation and migration of LUSC. By Figdraw.

and ATP production levels in NCI-H2170 and NCI-520 cells (Fig. 7B). Inhibition of *MTFP1* expression also reduced the mRNA expression levels of *LDHA*, *HK2*, *GLUT1*, and *PKM2* in both cell lines (Fig. 7C), suggesting that *MTFP1* positively regulates glycolysis in cancer cells.

To investigate whether *MTFP1* promotes cancer cell proliferation and growth by regulating the glycolytic pathway, we treated NCI-H2170 and NCI-520 cells with 2-Deoxy-D-glucose (2-DG), an inhibitor of glycolysis, and assessed their growth and proliferation. Compared with the control group without 2-DG treatment, we found that NCI-H2170 and NCI-520 cells treated with 2-DG had a significant reduction in their proliferation ability, and the proliferation of *MTFP1* knockout cells did not change significantly (Fig. 7D–E, Figs. S2A–B). Moreover, colony formation and migration abilities of these cells were significantly impaired after 2-DG treatment, and *MTFP1* knockout cells had no significant change (Fig. 7F–G, Figs. S2C–D). These results suggest that *MTFP1* promotes cancer cell proliferation and migration by positively regulating the glycolytic pathway (Fig. 8). *MTFP1* is a promising target for lung squamous cell carcinoma therapy.

4. Discussion

Lung squamous cell carcinoma has a poor survival prognosis due to the lack of effective therapeutic means [16]. Therefore, research on new targets and combination therapy, such as immunotherapy, is important. To achieve this, it is essential to study the molecular characteristics of lung squamous cell carcinoma. *MTFP1* is a nuclear coding protein that promotes mitochondrial division and is associated with the development of different types of cancer [17]. Abnormal overexpression of *MTFP1* was found in LUSC, which promoted the proliferation and migration of LUSC cells by activating the glycolysis pathway. *MTFP1* was overexpressed in LUSC according to TCGA, GEO, and PDC databases. High expression of *MTFP1* was associated with poor prognosis in LUSC patients. *MTFP1* was also found to be closely related to hypoxia and key enzymes of glycolysis in LUSC, which is a major marker of metabolic reprogramming in cancer [18]. *MTFP1* was found to be a new target gene of *HIF1A* and promoted the proliferation and growth of lung squamous cell cells.

To further explore the specific action mechanism of *MTFP1* in promoting LUSC, functional enrichment analysis was conducted using *MTFP1* co-expressed gene set and TCGA-LUSC sample data. The results revealed that *MTFP1* was mainly involved in ATP metabolism and glycolysis in LUSC. *MTFP1* was found to be significantly correlated with both glycolysis and oxidative phosphorylation, which are two pathways that primarily power tumor growth [19]. Silencing *MTFP1* expression led to reduced glycolysis in two types of lung squamous cell cells. This indicates that *MTFP1* promotes the development of LUSC by regulating the glycolysis pathway.

Of course, this study also has some limitations. Firstly, this study only investigated the *HIF1A* positive regulation of *MTFP1* induced by hypoxia, and further exploration of other genes regulated by *HIF1A* can be conducted. Secondly, this study only focused on the glycolytic pathway activated by *MTFP1*, while the occurrence and development of LUSC is a complex process, and further studies are needed to investigate other mechanisms of action. Finally, this study is a single-gene study, which does not provide a comprehensive understanding of the genetic variation of LUSC, so further genome-wide studies may be needed.

In conclusion, this study provides evidence that *MTFP1* is a novel target gene of *HIF1A* that promotes the growth of LUSC by activating the glycolysis pathway. It highlights the potential of *MTFP1* as a therapeutic target for LUSC patients who lack oncogene-targeted therapy. The findings also provide insight into the molecular features of LUSC, which may contribute to the development of novel effective targeted therapeutic agents for patients with lung squamous cell carcinoma who lack oncogene targeting therapy.

Funding

This study was supported by the National Natural Science Foundation of China (82104174 and 82273167), Jiangsu Province Basic Research Program Natural Science Foundation (Outstanding Youth Fund Project, BK20220063), the Key Program of Basic Science (Natural Science) of Jiangsu Province, (22KJA350001), "Huaguo Mountain Talent Plan" of Lianyungang City (Innovative Talents Liu Bin), Qing Lan Project of Jiangsu Universities (Outstanding young backbone teachers, Ji Jing), Priority Academic Program Development of Jiangsu Higher Education Institutions.

CRediT authorship contribution statement

Jing Ji: Writing – review & editing, Writing – original draft, Visualization, Supervision, Resources, Project administration, Methodology, Investigation, Funding acquisition, Formal analysis, Data curation, Conceptualization. **Yasong Wang:** Writing – review & editing, Writing – original draft, Visualization, Validation, Software, Data curation. **Aixin Jing:** Writing – original draft, Validation. **Ling Ma:** Validation, Data curation. **Jiayan Yang:** Validation. **Dexu Ren:** Writing – original draft, Visualization, Software, Data curation, Conceptualization. **Jinyu Lv:** Validation. **Mingxiao Lv:** Validation. **Menghan Xu:** Validation. **Qing Yuan:** Validation. **Xinhui Ma:** Validation. **Qilan Qian:** Validation. **Weiling Wang:** Validation. **Ting Geng:** Validation. **Yuanyuan Ding:** Validation. **Jingting Qin:** Validation. **Yuanyuan Liu:** Validation. **Jiaojiao Zhou:** Validation. **Lingyi Zuo:** Validation. **Shaojie Ma:** Resources, Project administration, Methodology. **Xiujun Wang:** Resources, Project administration, Methodology. **Bin Liu:** Writing – review & editing, Writing – original draft, Visualization, Supervision, Resources, Project administration, Methodology, Investigation, Funding acquisition, Formal analysis, Data curation, Conceptualization.

Declaration of competing interest

The authors declare that they have no known competing financial interests or personal relationships that could have appeared to influence the work reported in this paper.

Appendix A. Supplementary data

Supplementary data to this article can be found online at <https://doi.org/10.1016/j.heliyon.2024.e28440>.

References

- [1] H. Sung, J. Ferlay, R.L. Siegel, M. Laversanne, I. Soerjomataram, A. Jemal, F. Bray, Global cancer statistics 2020: GLOBOCAN estimates of incidence and mortality worldwide for 36 cancers in 185 Countries, *CA Cancer J Clin* 71 (2021) 209–249.
- [2] A.G. Nicholson, M.S. Tsao, M.B. Beasley, A.C. Borczuk, E. Brambilla, W.A. Cooper, S. Dacic, D. Jain, K.M. Kerr, S. Lantuejoul, M. Noguchi, M. Papotti, N. Rekhtman, G. Scagliotti, P. van Schil, L. Sholl, Y. Yatabe, A. Yoshida, W.D. Travis, The 2021 WHO classification of lung tumors: impact of advances since 2015, *J. Thorac. Oncol.* 17 (2022) 362–387.
- [3] E.S. Santos, E. Rodriguez, Treatment considerations for patients with advanced squamous cell carcinoma of the lung, *Clin. Lung Cancer* 23 (6) (2022 Sep) 457–466.
- [4] J. Liu, Y. Wang, J. Yin, Y. Yang, R. Geng, Z. Zhong, S. Ni, W. Liu, M. Du, H. Yu, J. Bai, Pan-cancer analysis revealed SRSF9 as a new biomarker for prognosis and immunotherapy, *J Oncol* 2022 (2022) 3477148.
- [5] Y. Liu, C. Chen, X. Wang, Y. Sun, J. Zhang, J. Chen, Y. Shi, An Epigenetic role of Mitochondria in cancer, *Cells* 11 (16) (2022) 2518.
- [6] K. Klein, K. He, A.I. Younes, H.B. Barsoumian, D. Chen, T. Ozgen, S. Mosaffa, R.R. Patel, M. Gu, J. Novaes, A. Narayanan, M.A. Cortez, J.W. Welsh, Role of Mitochondria in cancer Immune evasion and potential therapeutic approaches, *Front. Immunol.* 11 (2020) 573326.
- [7] B. Zhang, C. Pan, C. Feng, C. Yan, Y. Yu, Z. Chen, C. Guo, X. Wang, Role of mitochondrial reactive oxygen species in homeostasis regulation, *Redox Rep. : communications in free radical research* 27 (1) (2022) 45–52.
- [8] E. Donnarumma, M. Kohlhaas, E. Vimont, E. Kornobis, T. Chaze, Q.G. Gianetto, M. Matondo, M. Moya-Nilges, C. Maack, T. Wai, Mitochondrial Fission Process 1 controls inner membrane integrity and protects against heart failure, *Nat. Commun.* 13 (1) (2022 Nov 4) 6634.
- [9] D.P. Panigrahi, S. Patra, B.P. Behera, P.K. Behera, S. Patil, B.S. Patro, L. Rout, I. Sarangi, S.K. Bhutia, MTP18 inhibition triggers mitochondrial hyperfusion to induce apoptosis through ROS-mediated lysosomal membrane permeabilization-dependent pathway in oral cancer, *Free Radic. Biol. Med.* 190 (2022) 307–319.
- [10] Y. Zhang, H. Li, H. Chang, L. Du, J. Hai, X. Geng, X. Yan, MTP18 overexpression contributes to tumor growth and metastasis and associates with poor survival in hepatocellular carcinoma, *Cell Death Dis.* 9 (2018) 956.
- [11] T.T.T. Phan, Y.C. Lin, Y.T. Chou, C.W. Wu, L.Y. Lin, Tumor suppressor p53 restrains cancer cell dissemination by modulating mitochondrial dynamics, *Oncogenesis* 11 (2022) 26.
- [12] M.A. Applebaum, A.R. Jha, C. Kao, K.M. Hernandez, G. DeWane, H.R. Salwen, A. Chlenski, M. Dobratic, C.J. Mariani, L.A. Godley, N. Prabhakar, K. White, B. E. Stranger, S.L. Cohn, Integrative genomics reveals hypoxia inducible genes that are associated with a poor prognosis in neuroblastoma patients, *Oncotarget* 7 (47) (2016 Nov 22) 76816–76826.
- [13] S.C. Winter, F.M. Buffa, P. Silva, C. Miller, H.R. Valentine, H. Turley, K.A. Shah, G.J. Cox, R.J. Corbridge, J.J. Homer, B. Musgrove, N. Slevin, P. Sloan, P. Price, C.M. West, A.L. Harris, Relation of a hypoxia metagene derived from head and neck cancer to prognosis of multiple cancers, *Cancer Res.* 67 (7) (2007 Apr 1) 3441–3449.
- [14] A. Eustace, N. Mani, P.N. Span, J.J. Irlam, J. Taylor, G.N. Betts, H. Denley, C.J. Miller, J.J. Homer, A.M. Rojas, P.J. Hoskin, F.M. Buffa, A.L. Harris, J. H. Kaanders, C.M. West, A 26-gene hypoxia signature predicts benefit from hypoxia-modifying therapy in laryngeal cancer but not bladder cancer, *Clin. Cancer Res.* 19 (17) (2013 Sep 1) 4879–4888.
- [15] H.L. Jiao, B.S. Weng, S.S. Yan, Z.M. Lin, S.Y. Wang, X.P. Chen, G.H. Liang, X.Q. Li, W.Y. Zhao, J.Y. Huang, D. Zhang, L.J. Zhang, F.Y. Han, S.N. Li, L.J. Chen, J. H. Zhu, W.F. He, Y.Q. Ding, Y.P. Ye, Upregulation of OSBPL3 by HIF1A promotes colorectal cancer progression through activation of RAS signaling pathway, *Cell Death Dis.* 11 (7) (2020 Jul 24) 571.
- [16] J.W. Chen, J. Dhahbi, Lung adenocarcinoma and lung squamous cell carcinoma cancer classification, biomarker identification, and gene expression analysis using overlapping feature selection methods, *Sci. Rep.* 11 (1) (2021 Jun 25) 13323.
- [17] D. Tondera, A. Santel, R. Schwarzer, S. Dames, K. Giese, A. Klippel, J. Kaufmann, Knockdown of MTP18, a novel phosphatidylinositol 3-kinase-dependent protein, affects mitochondrial morphology and induces apoptosis, *J. Biol. Chem.* 279 (30) (2004 Jul 23) 31544–31555.
- [18] J. Yang, B. Ren, G. Yang, H. Wang, G. Chen, L. You, T. Zhang, Y. Zhao, The enhancement of glycolysis regulates pancreatic cancer metastasis, *Cell. Mol. Life Sci.* 77 (2) (2020 Jan) 305–321.
- [19] V. Sica, J.M. Bravo-San Pedro, G. Stoll, G. Kroemer, Oxidative phosphorylation as a potential therapeutic target for cancer therapy, *Int. J. Cancer* 146 (1) (2020 Jan 1) 10–17.